Applied Mathematics Letters 112 (2021) 106746

Contents lists available at ScienceDirect

Applied Mathematics Letters

www.elsevier.com/locate/aml

A regularized method of moments for three-dimensional time-harmonic electromagnetic scattering

Junpu Li [a,*], Lan Zhang [a,*], Qing-Hua Qin [b]

[a] *School of mechanics and safety engineering, Zhengzhou University, Zhengzhou, Henan 450001, China*
[b] *College of Engineering and Computer Science, Australian National University, Canberra ACT 2601, Australia*

ARTICLE INFO

Article history:
Received 22 July 2020
Received in revised form 3 September 2020
Accepted 3 September 2020
Available online 21 September 2020

Keywords:
Time-harmonic electromagnetic field
Electric field integral equation
Radar cross section
Method of moments
Origin intensity factor

ABSTRACT

A regularized method of moments based on the modified fundamental solution of the Helmholtz equation is proposed in this article. The regularized method of moments uses the origin intensity factor technique which is free of mesh and integration to deal with the singularity at origin of the basis function. Thus, the time-consuming singular integration can be avoided. In addition, the non-uniqueness at internal resonance is also fixed using the constructed modified fundamental solution. In comparison with the traditional method of moments, the regularized method of moments can reduce the computational time by half, while the stability and accuracy stay about the same. Numerical experiments demonstrate that the regularized method of moments can accurately and efficiently compute the radar cross section of perfect conducting scatter in all frequency ranges.

1. Introduction

Efficiently computing the radar cross section (RCS) [1] of the perfect conducting scatter is a hot topic in fields of computational electromagnetics [2]. Among computational methods reported in the literature, the method of moments (MOM) [3] is the most widely used method for electromagnetic problems. However, the traditional MOM would suffer the deficiencies of singularity at origin and non-uniqueness at internal resonance. In general, the singular integration is applied to deal with the singularity at origin of the fundamental solution. The electric field integral equation (EFIE) is combined with the magnetic field integral equation (MFIE) to fix the non-uniqueness at resonance frequency, i.e., the combined field integral equation (CFIE) [4]. However, both the two strategies would significantly increase the computing cost [5]. As is known to all, the matrix of the MOM is fully populated. Therefore, how to evaluate the RCS by the MOM with lower amount of calculation is a key task for computational electromagnetics.

* Corresponding authors.
E-mail addresses: junpu.li@foxmail.com (J. Li), ielzhang@zzu.edu.cn (L. Zhang).

https://doi.org/10.1016/j.aml.2020.106746
0893-9659/

In this letter, a regularized method of moments (RMOM) is constructed to accurately evaluate the RCS of perfect conducing scatter. In the RMOM, a modified fundamental solution of the three-dimensional (3-D) Helmholtz equation [6] which satisfies the radiation condition at infinity is constructed to fix the non-uniqueness at internal resonance. Compared to CFIE, the computational cost of the RMOM is reduced almost by half. As demonstrated in the subsequent examples, the RMOM can accurately generate the unique solution at any specified frequency. Furthermore, the origin intensity factor (OIF) technique [7–9] which is free of mesh and integration is used to deal with the singularity at origin of the modified fundamental solution. Therefore, the time-consuming singular integration is also avoided.

2. The regularized method of moments for electromagnetic scattering problems

The scattered electric field of a perfect conducting scatter is evaluated by the following equation

$$\overline{E}^{S} = i\omega\overline{A} - \nabla\varPhi, \tag{1}$$

where $\overline{E}^{S}$ is the scattered electric field, $\overline{A}$ the magnetic vector potential, $\varPhi$ the scalar potential, and ω the angular frequency. A bar over a variable represents that variable is a vector.

The perfect electric conductor (PEC) boundary condition is expressed as

$$-\overline{E}^{I}_{\tan} = (i\omega\overline{A} - \nabla\varPhi)_{\tan}, \tag{2}$$

where the subscript tan represents the tangential component. $\overline{E}^{I}$ is the incident electric field. $k = \omega\sqrt{\mu\varepsilon} = 2\pi/\lambda$, where k is the wave number, λ the wavelength. $\mu = 4\pi \times 10^{-7}$ and $\varepsilon = 8.854187817 \times 10^{-12}$ are the permeability and the permittivity of the surrounding free space.

In the RMOM, the RWG vector basis function $\overline{f}_n$ is used as the test function. With the symmetric product definition

$$\langle \overline{f}, \overline{g} \rangle = \int_S \overline{f} \cdot \overline{g} ds, \tag{3}$$

the interpolation matrix of the RMOM satisfies

$$\left\langle \overline{E}^{I}, \overline{f}_m \right\rangle = -i\omega \left\langle \overline{A}, \overline{f}_m \right\rangle + \left\langle \nabla\varPhi, \overline{f}_m \right\rangle \tag{4}$$

by testing Eq. (2) with $\overline{f}_n$, where $\overline{f}_n$ is the RWG vector basis function [3] associated with the nth edge as depicted in Fig. 1,

$$\overline{f}_n(\overline{r}) = \begin{cases} \dfrac{l_n}{2A_n^{+}}\overline{\rho}_n^{+}, \overline{r} \in T_n^{+} \\ \dfrac{l_n}{2A_n^{-}}\overline{\rho}_n^{-}, \overline{r} \in T_n^{-} \\ 0, \text{otherwise} \end{cases} \text{ and } \nabla_S \cdot \overline{f}_n = \begin{cases} \dfrac{l_n}{A_n^{+}}, \overline{r} \in T_n^{+} \\ -\dfrac{l_n}{A_n^{-}}, \overline{r} \in T_n^{-} \\ 0, \text{otherwise} \end{cases}. \tag{5}$$

The last term of Eq. (4) satisfies the following relationship

$$\left\langle \nabla\varPhi, \overline{f}_m \right\rangle = -\int_S \varPhi \nabla_S \cdot \overline{f}_m dS. \tag{6}$$

By expanding the induced surface currents $\overline{J}$ with

$$\overline{J} = \sum_{n=1}^{N} I_n \overline{f}_n(\overline{r}), \tag{7}$$

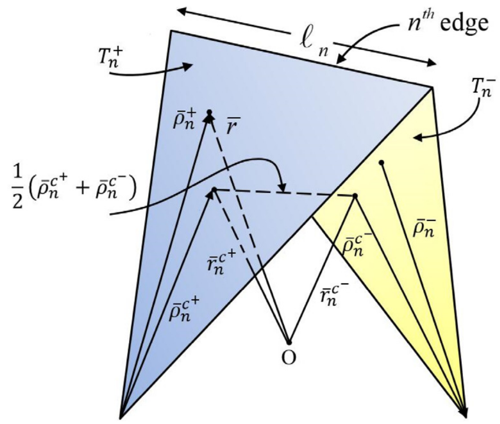

Fig. 1. RWG vector basis function.

Eq. (4) is reformulated as

$$ZI = V, \tag{8}$$

where

$$Z_{mn} = l_m \left[-i\omega \left(\overline{A}_{mn}^{+} \cdot \frac{\overline{\rho}_m^{c+}}{2} + \overline{A}_{mn}^{-} \cdot \frac{\overline{\rho}_m^{c-}}{2} \right) - \Phi_{mn}^{+} + \Phi_{mn}^{-} \right], \tag{9}$$

$$V_m = l_m \left(\overline{E}_m^{+} \cdot \frac{\overline{\rho}_m^{c+}}{2} + \overline{E}_m^{-} \cdot \frac{\overline{\rho}_m^{c-}}{2} \right), \overline{E}_m^{\pm} = \overline{E}^{I}(\overline{r}_m^{c\pm}), \tag{10}$$

$$\overline{A}_{mn}^{\pm} = \frac{\mu}{4\pi} \int_S \overline{f}_n(\overline{r}') M_m^{\pm}(\overline{r}') dS' \text{ and } \Phi_{mn}^{\pm} = \frac{1}{4\pi i\omega\varepsilon} \int_S \nabla'_S \cdot \overline{f}_n(\overline{r}') M_m^{\pm}(\overline{r}') dS', \tag{11}$$

In the MOM, the basis function is $G = e^{ikR}/R, R = |\overline{r} - \overline{r}'|$ [10]. However, the MOM would fail at internal resonance frequency due to the non-uniqueness of the solution. To remedy this drawback, the RMOM constructs a modified fundamental solution of the 3-D Helmholtz equation as the basis function as:

$$M = \alpha \frac{e^{ikR}}{R} + (1-\alpha) \frac{e^{i(kR-\pi/2)}}{R} = [\alpha - (1-\alpha)i] \frac{e^{ikR}}{R}, R = |\overline{r} - \overline{r}'|, \tag{12}$$

where $\alpha \in [0,1]$ is the shape parameter. The purpose of constructing the modified fundamental solution is to overcome the non-uniqueness at internal resonance frequency without increasing the amount of calculation.

The modified fundamental solution would suffer singularity when $R \to 0$. The RMOM uses the origin intensity factor technique given in Ref. [7] to deal with the singularity at origin of the modified fundamental solution. The OIF of the RMOM is written as

$$G_0 = -\frac{1}{kA_i} \sum_{j=1\neq i}^{N} \left[\begin{array}{l} kG(x_i, y_j) \displaystyle\sum_{m=1}^{3} \cos\left(k(y_m^j - x_m^i)\right) \cdot n^e(x_m^i) \cdot n^e(y_m^j) \\ -\dfrac{\partial G(x_i, y_j)}{\partial n^e(y_j)} \displaystyle\sum_{m=1}^{3} \sin\left(k(y_m^j - x_m^i)\right) \cdot n^e(x_m^i) \end{array} \right] A_j, \forall x_i \in S, \tag{13}$$

$$M_0 = [\alpha - (1-\alpha)i]\, G_0, \tag{14}$$

where $n^e(x_i) = \left(n^e(x_1^i), n^e(x_2^i), n^e(x_3^i)\right)$ and $n^e(y_j) = \left(n^e(y_1^j), n^e(y_2^j), n^e(y_3^j)\right)$ are the outer normal vector at source point x_i and observation point y_j, respectively. A_m is the area of range of influence of the mth source point.

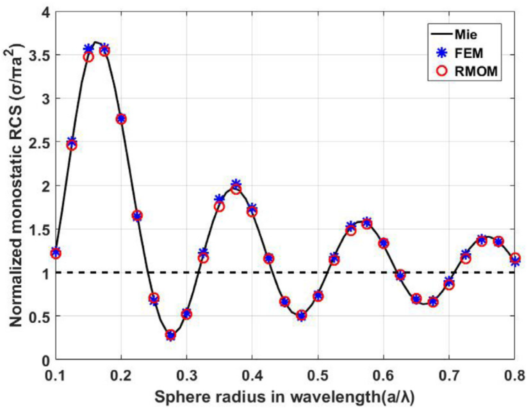

Fig. 2. Normalized monostatic RCS for sphere.

After the unknown coefficient vector I is obtained, the far-field scattered electric field can be approximately computed by

$$\overline{E}^S(\overline{r}) \approx [\alpha - (1-\alpha)i] \frac{i\omega\mu e^{ik|\overline{r}|}}{4\pi|\overline{r}|} \int_S J(\overline{r}')e^{-ik|\overline{r}'|\cdot\hat{r}} dS', \tag{15}$$

where $\hat{r} = \overline{r} - \overline{r}'/|\overline{r} - \overline{r}'| \approx \overline{r}/|\overline{r}|$, $\overline{r}'$ and $\overline{r}$ represent the coordinate of source point and observation point, respectively.

The radar cross section (RCS) is expressed as

$$\sigma_{3-D} = \lim_{r\to\infty} 4\pi r^2 \left|\overline{E}^S\right|^2 \Big/ \left|\overline{E}^I\right|^2 \text{ or } \sigma_{dBsm} = 10\lg(\sigma), \tag{16}$$

3. Numerical experiments

Example. Consider a perfect conducting sphere illuminated by an incident electric field $\overline{E}^I = (e^{ikz}, 0, 0)$. The plane electric wave travels in the $+Z$ direction with the electric field polarized along the X-axis. In this study, the shape parameter of the RMOM is $\alpha = 0.5$.

Case 1. The normalized monostatic RCS for perfect conducting sphere is investigated by the RMOM as plotted in Fig. 2. The Mie solution which is taken from Eq. (11–247) of Ref. [11] is expressed as

$$\sigma = \frac{\lambda^2}{4\pi}\left|\sum_{n=1}^{\infty} \frac{(-1)^n(2n+1)}{\hat{H}_n^{(2)'}(ka)\hat{H}_n^{(2)}(ka)}\right|^2. \tag{17}$$

Fig. 2 represents the lower half of a "Mie region" between the "Rayleigh region" and the "Optics region". It can be observed that there is in good agreement between the RMOM solution and the Mie solution.

Case 2. The non-uniqueness at internal resonance is investigated in this case. The Galerkin discretization suffers the first spherical resonance at $ka = 2.769$ and the second spherical resonance at $ka = 4.518$. Fig. 3 depicts the bistatic RCS of a resonant sphere at $ka = 2.769$, where sphere radius $a = 1$ m. The degrees of freedom (DOF) of the RMOM are 2794. In Fig. 3, the RMOM solution is compared to the EFIE solution and the Mie solution which are given in Ref. [4]. The monostatic RCS computed by the RMOM and the related computing data given in Ref. [12] are listed in Table 1 and Table 2, where $ka = 2.769$ and $ka = 4.518$, respectively.

Figs. 3a and 3b are called horizontal and vertical polarization RCS, respectively. As expected, the EFIE solution fails entirely at the spherical resonance frequency, while the RMOM solution is in good agreement

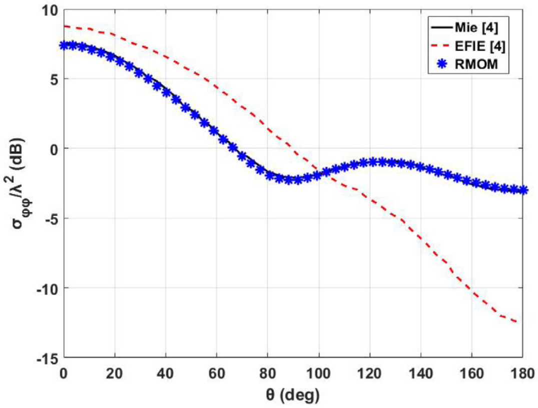

Fig. 3a. Bistatic RCS for the conducting sphere at internal resonance $ka = 2.768$.

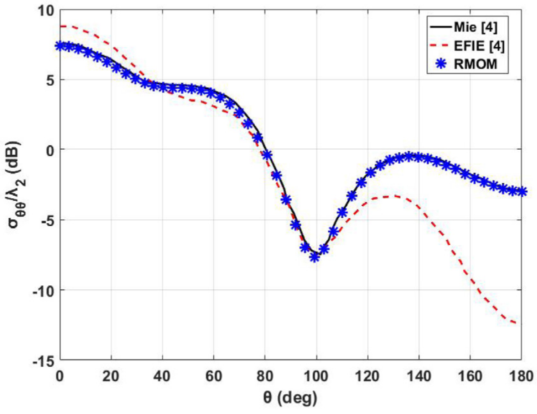

Fig. 3b. Bistatic RCS for the conducting sphere at internal resonance $ka = 2.768$.

Table 1
Resonant sphere monostatic RCS when $ka = 2.768$ ($\theta = 180°$).

Method	Mie	RMOM ($\alpha = 0.5$)	EFIE [12]	CFIE ($\alpha = 0.5$) [12]
σ/λ^2(dB)	−2.88	−2.97	−12.48	−3.07
ERROR		3.13%		6.60%

Table 2
Resonant sphere monostatic RCS when $ka = 4.518$ ($\theta = 180°$).

Method	Mie	RMOM ($\alpha = 0.5$)	EFIE [12]	CFIE ($\alpha = 0.5$) [12]
σ/λ^2(dB)	2.68	2.63	5.53	2.66
ERROR		1.87%		0.75%

with the Mie solution. It is demonstrated that the RMOM successfully fixes the problem of non-uniqueness at internal resonance frequency by using the modified fundamental solution as the basis function.

Case 3. The numerical efficiency of the RMOM is investigated. In this case, the frequency of incident wave is 600 MHz. The experimental data of the normalized monostatic RCS by the RMOM, the finite element method (FEM) [13–16] and the singular boundary method (SBM) [17–20] are listed in Table 3, where the experimental data of the FEM and the SBM is taken from Ref. [21].

Table 3
Normalized monostatic RCS by the FEM, the SBM and the RMOM.

FEM [21]			SBM [21]			RMOM		
DOF	Error	CPU (s)	DOF	Error	CPU (s)	DOF	Error	CPU (s)
200 559	2.85%	313	3200	2.14%	49	3216	2.51%	17.86
380 008	1.96%	633	5000	1.69%	183	5010	1.57%	43.59

It is observed that the RMOM only requires less than half of the CPU time consumed by the SBM to generate the similar solution. In comparison with the FEM solution which is computed by the COMSOL, the computing time of the RMOM is only its one tenth or even less.

4. Conclusions

In this letter, a regularized method of moments is proposed to accurately evaluate the RCS for perfect conducting scatter. The main purpose of the RMOM is to remedy two deficiencies of the MOM while maintaining its efficiency and accuracy, i.e., the singularity at origin of the basis function and the non-uniqueness at internal resonance. The RMOM uses the OIF to deal with the singularity at origin of the modified fundamental solution, which avoids the time-consuming singular integration. The RMOM uses the modified fundamental solution as the basis function, which overcomes the difficulty of non-uniqueness without increasing the computational and storage complexity. Experiments show that the RMOM can accurately evaluate the RCS for all frequency with much lower amount of cost of calculation and then the CPU time than those of the CFIE due to the application of the two proposed techniques.

CRediT authorship contribution statement

Junpu Li: Conceptualization, Software, Methodology, Writing - original draft. **Lan Zhang:** Writing - review & editing. **Qing-Hua Qin:** Writing - review & editing.

Acknowledgment

The work was supported by the Fundamental Research Funds for the Central Universities, China (Grant Nos. 2018B40714).

References

[1] W.C. Gibson, The Method of Moments in Electromagnetics, Chapman and Hall/CRC, New York, 2007.
[2] J.P. Li, W. Chen, Q.H. Qin, Z.J. Fu, A modified multilevel algorithm for large-scale scientific and engineering computing, Comput. Math. Appl. 77 (2019) 2061–2076.
[3] S. Rao, D. Wilton, A. Glisson, Electromagnetic scattering by surfaces of arbitrary shape, IEEE Trans. Antennas Propag. 30 (1982) 409–418.
[4] P. Huddleston, L. Medgyesi-Mitschang, J. Putnam, Combined field integral equation formulation for scattering by dielectrically coated conducting bodies, IEEE Trans. Antennas Propag. 34 (1986) 510–520.
[5] Z.J. Fu, S. Reutskiy, H.G. Sun, J. Ma, M.A. Khan, A robust kernel-based solver for variable-order time fractional PDEs under 2D/3D irregular domains, Appl. Math. Lett. 94 (2019) 105–111.
[6] J.P. Li, W. Chen, A modified singular boundary method for three-dimensional high frequency acoustic wave problems, Appl. Math. Model. 54 (2018) 189–201.
[7] J.P. Li, Z.J. Fu, W. Chen, Q.H. Qin, A regularized approach evaluating origin intensity factor of singular boundary method for Helmholtz equation with high wavenumbers, Eng. Anal. Bound. Elem. 101 (2019) 165–172.
[8] J.P. Li, W. Chen, Z.J. Fu, Q.H. Qin, A regularized approach evaluating the near-boundary and boundary solutions for three-dimensional Helmholtz equation with wideband wavenumbers, Appl. Math. Lett. 91 (2019) 55–60.
[9] J.P. Li, Z.J. Fu, W. Chen, Numerical investigation on the obliquely incident water wave passing through the submerged breakwater by singular boundary method, Comput. Math. Appl. 71 (2016) 381–390.

[10] L.C. Chen, X.L. Li, Boundary element-free methods for exterior acoustic problems with arbitrary and high wavenumbers, Appl. Math. Model. 72 (2019) 85–103.
[11] C.A. Balanis, Advanced Engineering Electromagnetics, John Wiley & Sons, New York, 1989.
[12] L. Medgyesi-Mitschang, D.S. Wang, Hybrid solutions at internal resonances, IEEE Trans. Antennas Propag. 33 (1985) 671–674.
[13] W.Z. Qu, A high accuracy method for long-time evolution of acoustic wave equation, Appl. Math. Lett. 98 (2019) 135–141.
[14] Y. Gu, C.M. Fan, R.P. Xu, Localized method of fundamental solutions for large-scale modelling of two-dimensional elasticity problems, Appl. Math. Lett. 93 (2019) 8–14.
[15] Y.B. Chai, C. Cheng, W. Li, Yu Huang, A hybrid Finite element-Meshfree method based on partition of unity for transient wave propagation problems in homogeneous and inhomogeneous media, Appl. Math. Model. 85 (2020) 192–209.
[16] J. Jirousek, Q.H. Qin, Application of hybrid-Trefftz element approach to transient heat conduction analysis, Comput. Struct. 58 (1996) 195–201.
[17] F.J. Wang, Y. Gu, W.Z. Qu, C.Z. Zhang, Localized boundary knot method and its application to large-scale acoustic problems, Comput. Methods Appl. Mech. Engrg. 361 (2020) 112729.
[18] J. Lin, Y. Xu, Y.H. Zhang, Simulation of linear and nonlinear advection-diffusion-reaction problems by a novel localized scheme, Appl. Math. Lett. 99 (2020) 106005.
[19] J.P. Li, Z.J. Fu, W. Chen, X.T. Liu, A dual-level method of fundamental solutions in conjunction with kernel-independent fast multipole method for large-scale isotropic heat conduction problems, Adv. Appl. Math. Mech. 11 (2019) 501–517.
[20] L.L. Sun, C. Zhang, Y. Yu, A boundary knot method for 3D time harmonic elastic wave problems, Appl. Math. Lett. 104 (2020) 106210.
[21] X. Wei, L.L. Sun, Singular boundary method for 3D time-harmonic electromagnetic scattering problems, Appl. Math. Model. 76 (2019) 617–631.